CHAPTER VII
ROOM TEMPERATURE SYNTHESIS OF Mo-SBA-15 VIA SOL-GEL PROCESS AND ITS CATALYTIC ACTIVITY IN STYRENE OXIDATION

7.1 Abstract

A series of molybdenum-substituted mesoporous SBA-15 (Mo-SBA-15) silicas with various Mo/Si mole ratios were synthesized at room temperature by a sol-gel process from moisture stable silatrane and molybdenum glycolate as metal sources, and a non-ionic triblock copolymer ($EO_{20}PO_{70}EO_{20}$) as a template. Small angle X-ray scattering (SAXS), transmission electron microscopy (TEM) and field emission scanning electron microscopy (FESEM) revealed a highly ordered *p6mm* hexagonal mesoporous structure. Diffuse reflectance UV-visible spectroscopy (DRUV) indicated that the incorporation of Mo^{6+} into the SBA-15 framework was optimal at 1.0 mol% molybdenum, beyond which extra-framework MoO_3 forms. N_2 adsorption/desorption measurements showed high surface areas (up to 729 m^2/g), with large pore diameters (6.8 nm) and volumes (1.04 cm^3/g). Mo-SBA-15 showed high catalytic activity for the epoxidation of styrene monomer with hydrogen peroxide (H_2O_2). The products of this reaction were styrene oxide and benzaldehyde.

(Keywords: Mo-SBA-15, silatrane, molybdenum glycolate, sol-gel process, styrene epoxidation)

7.2 Introduction

Since researchers from the Mobil Research and Development Corporation reported the M41S family of mesoporous silicas [1-2], much effort has been devoted to simplify the synthesis and expand to application of mesoporous molecular sieves. In particular, SBA-15 prepared using a non-ionic triblock copolymer as template is of interest due to its narrow pore size distribution [3] that leads to uniform hexagonal arrangement of channels (5-30 nm). A large internal surface area (600-1000 m^2/g) creates a large number of dispersed catalytically active centers, while the thick

framework walls (~3-7 nm) possess a hydrothermal stability exceeding that of thinner-walled MCM-41 materials [1-3]. However, pure silica SBA-15 is poorly catalytic due to the lack of lattice defect, limited redox properties, basicity and acidity. These limitations can be overcome by introducing guest species into the SBA-15 framework to improve the catalytic activity [4].

Zhao et al. [3] synthesized SBA-15 directly in acidic conditions from tetraethylorthosilicate (TEOS) and $EO_{20}PO_{70}EO_{20}$ as a template by hydrothermal treatment (100°C/48 h). Recently, Samran et al. [5] reported the room temperature sol-gel synthesis of SBA-15 using a silatrane precursor, and $EO_{20}PO_{70}EO_{20}$ as the structure directing agent. In both the direct method and sol-gel process, SBA-15 formed via $(S^0H^+)(X^-I^+)$ entities where S, X and I are the non-ionic surfactant, halide anion and protonated Si-OH, respectively [3,6].

Among various metal dopants, molybdenum-bearing catalysts show high activity for many reactions, such as propene metathesis [7-8], propene oxidation [9-11] and methanol oxidation [12]. The most widely used methods for preparing Mo-SBA-15 are post-synthesis impregnation [13] and direct synthesis [14]. For example, Mo-SBA-15 was prepared hydrothermally (100°C/24 h) by Melero et al. [15] using tetraethylorthosilicate (TEOS) and ammonium molybdate tetrahydrate ($(NH_4)_6(Mo_7O_{24}).4H_2O$) as the silica and molybdenum sources. In this paper, we report a simple and effective sol-gel route to directly incorporate molybdenum into the SBA-15 framework from moisture stable silatrane and molybdenum glycolate precursors, the reaction proceeds at room temperature rather than hydrothermally. The incorporation of molybdenum was characterized by small angle X-ray scattering (SAXS), transmission electron microscopy (TEM), field emission scanning electron microscopy (FESEM), diffuse reflectance UV-visible spectroscopy (DRUV), and N_2 adsorption. The catalytic activity of Mo-SBA-15 towards epoxidation of styrene monomer with H_2O_2 employed as the oxidant, was studied as a function of temperature, time, catalyst loading, Mo content and styrene:H_2O_2 ratio. The performance of catalysts synthesized via impregnation and sol-gel methods was compared.

7.3 Experimental section

7.3.1 Materials

Fumed silica (SiO_2, 99.8%) (Sigma-Aldrich, St. Louis, MO), triethanolamine (TEA) (Carlo Erba, Milan, Italy), ethylene glycol (EG) (J.T. Baker, Philipsburg, NJ), acetronitrile (Labscan, Bangkok, Thailand), molybdenum (VI) oxide (Fluka, Asia), poly(ethylene glycol)-block-poly(propylene glycol)-block-poly(ethylene glycol) ($EO_{20}PO_{70}EO_{20}$) (Sigma-Aldrich, Singapore), hydrochloric acid (HCl) (Labscan, Asia), hydrogen peroxide (H_2O_2) (Labscan, Asia), and styrene monomer (Labscan, Asia) were used without further purification.

7.3.2 Mo-SBA-15 sol-gel synthesis

Mo-SBA-15 was synthesized from silatrane and molybdenum glycolate as the silica and molybdenum sources, $EO_{20}PO_{70}EO_{20}$ as the structure-directing agent, and 2 M HCl was the acid catalyst. Different n_{Mo}/n_{Si} molar ratios were introduced according to the method of Samran et al. [5]. A solution of $EO_{20}PO_{70}EO_{20}$:HCl:silatrane:H_2O = 2:60:4.25:12 (mass ratio) was prepared by dissolving 4 g of $EO_{20}PO_{70}EO_{20}$ polymer in 80 g of 2 M HCl (part A) and 8.8 g of silatrane [16-17] in 20 g of H_2O (part B) with continuous stirring for 1 h to ensure complete dissolution. The solution of part B was then poured into part A. The required amount of molybdenum glycolate [18] was added to the homogenous solution with stirring. The resulting gel was aged at room temperature (RT) for 24 h and the product recovered by filtration, washed with deionized water, and dried at ambient overnight. This resin was calcined (550 °C/air/6 h) in a tube furnace (Carbolite, CFS 1200, Hope Valley, U.K.) at a heating rate of 0.5 °C/min to remove residual organics. The catalysts were designated as *(x)* mol% Mo-SBA-15 where *x* denotes the n_{Mo}/n_{Si} percentage used during synthesis. Molybdenum-free SBA-15 was synthesized using the same procedure ($EO_{20}PO_{70}EO_{20}$:HCl:silatrane:H_2O = 2:60:4.25:12) in the absence of molybdenum glycolate.

7.3.3 Impregnation synthesis

The incipient wetness impregnation method was used to deposit molybdenum on the SBA-15 support, using 1.0 and 1.25 mol% molybdenum

glycolate. The precursor was dissolved in water and dropped onto the catalyst supports. Drying (100 °C/12 h) was followed by calcination (550 °C/6 h) at a heating rate of 0.5 °C/min.

7.3.4 Characterization

The products were characterized by powder X-ray diffraction (XRD) with a PANalytical PW3830 instrument using CuKα (λ_{av}=0.154 nm) radiation generated at 50kV and 40 mA, over the 2θ range 0.5–10°, step size of 0.01° and dwell time of 10 seconds per step. Transmission electron microscopy (TEM) was conducted using a Hitachi H-7100FA machine operating at 125 kV with a large objective aperture. Field emission scanning electron microscopy (FESEM) was used to collect secondary electron images from powders mounted on double-sided carbon tape using a Zeiss Ultra plus, operating at 0.3-0.5 kV to minimize charging. Nitrogen adsoption and desorption isotherms were measured at -196 °C after outgassing at 250 °C for 12 h under vacuum (Quantasorb JR, Mount Holly, NJ) to determine the Brunauer–Emmett–Teller (BET) specific surface area. The pore size distributions were obtained from the adsorption and desorption branches of the nitrogen isotherms by the Barrett-Joyner-Halenda method. Diffuse reflectance UV-visible (DRUV) spectroscopic measurements were recorded on a Shimadzu UV-2550 spectrophotometer fitted with an ISR-2200 integrating sphere attachment and recorded from 190–600 nm and using $BaSO_4$ as a reference.

7.3.5 Catalytic activity

The epoxidation of styrene was measured from data collected in a batch reactor. The catalyst (0.05-0.20 g), styrene (5 mmol), hydrogen peroxide (2.5-10 mmol of 30 wt% aqueous solution) and acetronitrile (5 ml) were introduced to a glass flask with closed cap (30 ml). The reactant mixture was stirred and heated for a fixed time (6-48 h) and temperature (60-80 °C) in an oil bath. The products were identified and quantified by gas chromatography (GC) employing a capillary column (DB-Wax, 30 m x 0.25 mm) and flame ionization detector (FID). The conversion of styrene was calculated based upon the quantity of styrene monomer consumed.

7.4 Results and Discussion

7.4.1 Mesostructure and Crystal Chemistry

Pure SBA-15 and Mo-SBA-15 (0.25-1.25 mol% Mo) synthesized via sol-gel processing and calcined at 550°C gave the SAXS patterns shown in Figure 1. In all cases the two well-resolved scattering maxima at 2θ of 0.45° and 1.35° could be indexed to the {10} ≡ {11} and {30} ≡ {33} reflections, respectively. These scattering peaks are characteristic of *p6mm* symmetry and similar to pure silica SBA-15 [5]. This hexagonal motif was observed for all Mo-SBA-15 materials indicating that mesopore order was sustained after the introduction of molybdenum into the framework, due to the mild synthesis conditions employed and the extraordinarily high purity and moisture resistance of the silatrane precursor. The d-spacing (d_{10}) and the hexagonal translational parameter (a_0), increased significantly at 1.0 mol% Mo (Table 1). This may arise because the Mo-O bond length in either tetrahedral or octahedral coordination is longer than Si-O [19], indicative of Mo substitution, the increase in d_{10} and a_0 compared to the pure SBA-15 could confirm the incorporation of molybdenum species into the framework of SBA-15. As d_{10} and a_0 decrease for Mo content > 1.0 mol% an upper limit for framework incorporation is supposed under these synthetic conditions. The shift of d-spacings to smaller angles with increasing in Mo loading is analogous to other metal-substituted mesoporous materials [20]. Transmission electron micrograph (Figure 2) showed well aligned channel, confirming the long range ordered hexagonal structure of the synthesized materials.

Diffuse reflectance UV-vis (DRUV) spectrometry was used to extract coordination sphere and bonding information for calcined Mo-SBA-15 (0.25-1.25 mol% Mo) with all materials showing strong adsorption from 220-250 nm and at 290 nm (Figure 3). According to Cotton et al. [21], these bands are expected for ligand-metal charge transfer in oxomolybdates (O^{2-}-Mo^{6+}) with the position of the electronic transitions depending on ligand field symmetry surrounding the Mo center; tetrahedral Mo^{6+} (T_d) will show a higher energy transition than octahedral (O_h) [22]. Therefore, the 220-250 nm absorption is attributed to isolated tetrahedral Mo^{6+} species of mono- and dioxo molybdenum species, indicating that the MoO^{4-} species incorporated into the framework via Mo-O-Si bridge, due to the transition of an

oxygen 2pπ electron into the empty d-orbital of the molybdenum, consistent with Jezlorowski et al. [23]. The band at 290 nm refers to the electronic transitions of Mo-O-Mo bonds from molybdenum oligomer species [15]. The absorption tail at ~340-400 nm in the 1.25 mol% Mo sample suggests extra-framework trioxide MoO_3, that contains octahedral Mo^{6+} species (O_h (t_{2u},t_{1g}→t_{2g})) [24-25]. These results provide further confirmation that the upper limit of framework molybdenum incorporation in SBA-15 is < 1.0 mol%.

N_2 adsorption/desorption isotherms; all sample yield type IV isotherms (IUPAC classification) and exhibit broad H1 type hysteresis loops, typical of large-pore mesoporous solids. The corresponding pore size distribution curves derived from the desorption branch of the calcined Mo-SBA-15 are presented in Figure 4. The well-defined step at a relatively high pressure of 0.5–0.7 corresponds to capillary condensation of N_2 within uniform pores (> 5 nm diameter) and high surface area (up to 729 m^2/g) (Table 1). The synthesized Mo-SBA-15 catalysts exhibited large surface areas (607-729 m^2/g) and pore volumes (0.72-1.04 cm^3/g). However, the incorporation of molybdenum into the framework of SBA-15 to high molybdenum loadings (1.25 mol% Mo) has significant effect on the BET, pore volume, pore diameter and especially so for surface area, and could indicate the formation of extra-framework MoO_3 within the pores as suggested by DRUV.

7.4.2 Catalytic activity study of Mo-SBA-15

Catalytic activity towards epoxidation of styrene using H_2O_2 as an oxidant was tested in a batch-type reactor. At the end of the reaction the catalyst was separated by filtration and the products analyzed by gas chromatography (Table 2). A blank reaction performed over pure SBA-15 under identical conditions showed no catalytic activity. Hydrogen peroxide alone was also unable to oxidize styrene in the absence of mesoporous silica, whereas all Mo-SBA-15 samples were efficient catalysts. Styrene conversion increased with molybdenum content up to 1.0 mol% to a maximum of 6.3% with the selectivities for benzaldehyde and styrene oxide 70.9% and 29.1%, respectively. However, at 1.25 mol% Mo loading, conversion efficiency and selectivity of styrene oxide significantly decreased, consistent with extra-framework MoO_3 causing channel blockage that restricts the diffusion of styrene to

the tetrahedral molybdenum framework species where oxidation is likely to take place [19].

To provide a baseline for comparison, molybdenum was impregnated onto the SBA-15 framework and its catalytic activity studied. The impregnated material containing 1.0 mol% Mo showed lower styrene conversion (4.7%) than the equivalent catalyst obtained from sol-gel processing (6.3%); the poor dispersion and mesopore plugs of metal oxides appear responsible for the relatively poor catalytic activity of the former [26]. Additionally, the impregnated samples deliver lower styrene oxide selectivity (22.1%) than the catalyst prepared via sol-gel process (29.1%). This result agrees with Rana et al. [27] who reported that Mo-MCM-41 synthesized hydrothermally showed a higher activity for the oxidation of cyclohexane and gave a more stable cyclohexanol product, in comparison to the impregnated catalyst. This was attributed to the tetrahedral coordination of active molybdenum in the silica framework. The effect of reaction time was investigated in three stages from 6 h to 48 h (Table 3) and showed that at 48 h, styrene conversion increases significantly to 22.6% while styrene oxide selectivity substantially decreases to 7.5% with a corresponding increase in benzaldehyde selectivity of 92.5%. Benzaldehyde is produced during nucleophilic attack of styrene oxide by H_2O_2 followed by cleavage of the intermediate hydroxyl-hydroperoxistyrene [28]. As temperature increased from 60°C to 80°C, styrene conversion was enhanced to 42.1% at 80°C (Table 4), but selectivity of benzaldehyde increased at the cost of the styrene oxide, indicating that benzaldehyde forms mainly via further oxidation of styrene oxide, and that the higher temperature favors the oxidation of styrene oxide [19]. In contrast, the product obtained from the reaction temperature of 60°C was only benzaldehyde which could be formed from a radical mechanism through direct oxidative cleavage of the styrene side chain double bond [28]. The styrene conversion was greatly enhanced (9.1%) when the mole ratios of styrene: H_2O_2 are 1:1.5 (Table 3). With increasing styrene/H_2O_2 mole ratio, styrene conversion increased considerably due to improved H_2O_2 utilization, beyond which, no further was observed. The effect of catalyst loading in the batch reactor is shown in Table 6. Styrene conversion reached 6.3% when 0.05g of catalyst was used and did not

significantly change when compared with 0.10g and 0.15g. The maximum styrene oxide selectivity (39.9%) with reasonable styrene conversion (7.7%) was observed at 0.10g catalyst. Hence, the optimum catalyst used was 0.10g.

7.5 Conclusions

Mo-SBA-15 was synthesized via a sol-gel process using silatrane as the silica precursor, molybdenum glycolate as the molybdenum source, and a nonionic triblock copolymer ($EO_{20}PO_{70}EO_{20}$) as template. This room temperature synthesis is simple and avoids hydrothermal treatment as conventionally required. The catalysts maintained a *p6mm* hexagonal mesostructure, high surface area (729 m^2/g), large pore diameter (6.8 nm) and volume (1.04 cm^3/g). The optimal framework molybdenum loading into SBA-15 without separation of extra-framework MoO_3 while maintaining tetrahedral coordination is 1.0 mol%. In addition, these Mo-SBA-15 materials show relatively high catalytic activity for the epoxidation of styrene monomer with hydrogen peroxide due to the presence of molybdenum species in the SBA-15 framework. The product obtained from sol-gel synthesis provides superior catalytic activity compared to the impregnation method. The optimal condition for epoxidation of styrene over Mo-SBA-15 is 70°C for 24 hour, using 0.10 g catalyst containing 1.0 mol% Mo, and a 1:1 mol ratio of styrene:H_2O_2. The only products obtained are styrene oxide and benzaldehyde. The selectivity of styrene oxide and benzaldehyde reached 39.9% and 60.1% at a styrene conversion of 7.7%, and demonstrates that Mo-SBA-15 heterocatalyst can be synthesized by an inexpensive and energy saving process for a range of catalytic applications.

7.6 Acknowledgements

This research work is financially supported by the Postgraduate Education and Research Program in Petroleum and Petrochemical Technology (ADB) Fund (Thailand), the Ratchadapisake Sompote Fund, Chulalongkorn University, and the Thailand Research Fund (TRF). The SAXS patterns were collected by Mr. An Tao and Ms. Li Henan at the School of Materials Science and Engineering, Nanyang

Technological University. Dr. Frank Brink of the Australian National University collected the secondary electron images.

7.7 References

1. Kresge, C. T.; Leonowicz, M. E.; Roth, W. J.; Vartuli, J. C.; Beck, J. S. *Nature* **1992**, *359*, 710-712.
2. Beck, J. S.; Vartuli, J. C.; Roth, W. J.; Leonowicz, M. E.; Kresge, C. T.; Schmitt, K. D.; Chu, C. T. W.; Olson, D. H.; Sheppard, E. W.; McCullen, S. B.; Higgins, J. B.; Schlenker, J. L. *J. Am. Chem. Soc.* **1992**, *114*, 10834-10843.
3. Zhao, D.; Feng, J.; Huo, Q.; Melosh, N.; Frerickson, G. H.; Chmelka, B. F.; Stucky, G. D. *Science* **1998**, *279*, 548-552.
4. Xiao, F.-S. Top. Catal. **2005**, *35*, 9.
5. Samran, B.; White, T.J.; Wongkasemjit, S. *Journal of Porous Materials* **2010** DOI. 10.1007/s10934-010-9367-3
6. Zhao, D.; Huo, Q.; Feng, J.; Chmelka, B. F.; Stucky, G. D. *J. Am. Chem. Soc.* **1998**, *120*, 6024-6036.
7. Ono, T.; Anpo, M.; Kubokawa, Y. *J. Phys. Chem.* **1986**, *90*, 4780.
8. Liu, T-C.; Forissier, M.; Coudurier, G.; Ve´drine, J.C. *J. Chem. Soc. Faraday. Trans.* **1989**, *85*, 1607.
9. Giordano, N.; Meazza, M.; Castellan, A.; Bart. J.C.J.; Ragaini, V. *J. Catal* **1977**, *50*, 342.
10. Ressler, T.; Wienold, J.; Jentoft, R.E.; Girgsdies, F. *Eur. J. Inorg. Chem.* **2003**, *2*, 301.
11. Kotov, St.V.; Balbolov, E. *J. Mol. Catal. A* **2001**, *176*, 41–48.
12. Louis, C.; Tatibouet, J.-M.; Che, M. J. Catal. **1988**, *109*, 354.
13. Yang, Q.; Cope´ret, C.; Li, C., Basset, J.M. *New. J. Chem.* **2003**, *27*, 319–323.
14. Zhang, W.; Wangt, J.; Tanev, P.T.; Pinnavaia, T. *Chem. Commun.* **1996**, *69*, 79–980.
15. Melero, J.A.; Iglesias, J.; Arsuaga, J.M.; Sainz-Pardo, J.; de Frutos, P.; Blazquez, S. *J. Applied Catalysis A : General* **2007**, *331*, 84–94.

16. Phiriyawirut, P.; Magaraphan, R.; Jamieson, A. M.; Wongkasemjit, S. *Material Science and Engineering A* **2003**, *361*, 147-154.
17. Charoenpinijkarn, W.; Suwankruhasn, M.; Kesapabutr, B.; Wongkasemjit, S.; Jamieson, A. M. *European Polymer Journal* **2001**, *37*, 1441-1448.
18. Wongkasemjit, S.; Tamuang, S.; Tanglumlert, W.; Imae, T. *Materials Chemistry and Physics* **2009**, *117*, 301-306.
19. Ji, D.; Zhao, R.; Lv, G.; Qian, G.; Yan, L.; Suo, J. *Applied Catalysis A : General* **2005**, *281*, 39-45
20. Lui, C.; Chen, C.; Leu, J.; Lin, Y. *J. Sol-Gel Sci Techn* **2007**, *43*, 47-51.
21. Cotton, F.A.; Wilkinson, G. *Advance Inorganic Chemistry, 4th ed., John Wiley & Sons, New York,* **1980**.
22. Weber, R.S. *J. Catal.* **1995**, *151*, 470-474.
23. Jezlorowski, H.; Knozinger, H. *J. Phy. Chem.* **1979**, *83*, 1166-1173.
24. Higashimoto, S.; Hu, Y.; Tsumura, R.; Iino, K.; Matsuoka, M.; Yamashita, H.; Shul, Y.; Che, M.; Anpo, M. *J. Catal.* **2005**, *235*, 272-278.
25. Che, S.; Sakamoto, H.; Yoshitake, H.; Terasaki, O.; Tatsumi, T. *J. Phys. Chem. B* **2001**, *105*, 10565-10572.
26. Zhang, L.; Hua, Z.; Dong X.; Li, L.; Chen, H.; Shi, J. *Journal of molecular catalysis A: Chemical* **2007**, *268*, 155-162.
27. Rana, R.K.; Viswsabathan, B. *Catal. Lett.* **1998**, *52*, 25-29.
28. Hulea, V.; Dumitriu, E. *Applied Catalysis A : General* **2004**, *277*, 99-106.

Table 1. Physical and crystallographic properties of Mo-SBA-15 samples as a function of Mo loading

Sample	Physical properties				Crystallographic properties	
Loaded Mo (mol%)	Surface area (m^2/g) BET	Pore volume (cm^3/g) BET	Channel diameter (nm) BET	Channel diameter (nm) SAXS	d_{10}(nm) SAXS	a_0(nm) SAXS
Pure SBA-15	570	0.72	5.03	6.0-6.3	18.2	21.0
0.25	607	0.77	5.38	6.2-6.5	18.6	21.5
0.50	687	0.81	5.77	6.1-6.4	17.1	19.7
0.75	729	1.04	6.76	6.5-6.8	18.6	21.5
1.00	708	0.76	5.38	6.3-6.6	20.7	23.9
1.25	409	0.47	4.62	5.8-6.1	18.6	21.5

Table 2. Epoxidation of styrene monomer with H_2O_2 over Mo-SBA-15 as a function of Mo loading

Loaded Mo (mol %)	Styrene conversion (%)	Selectivity (%)	
		Benzaldehyde	Styrene oxide
Styrene and H_2O_2*	-	-	-
Pure SBA-15	-	-	-
0.25% Mo	5.7	75.1	24.9
0.50% Mo	5.5	65.2	34.8
0.75% Mo	5.8	77.6	27.6
1.00% Mo	6.3	70.9	29.1
1.25% Mo	4.4	81.0	19.0
1.00% Mo (impreg.)	4.7	77.9	22.1
1.25% Mo (impreg.)	4.2	80.9	19.1

*The reaction was conducted in the absence of mesoporous silica.

Reaction condition: catalyst 0.05 g/70 °C/24 h/styrene:H_2O_2 = 1:1

Table 3. Epoxidation of styrene monomer with H_2O_2 over Mo-SBA-15 as a function of reaction time

Time (h)	Styrene conversion (%)	Selectivity (%)	
		Benzaldehyde	Styrene oxide
6	4.2	72.3	27.7
24	6.3	70.9	29.1
48	22.6	92.5	7.5

Reaction condition: 0.05 g of 1.0 mol% Mo/styrene:H_2O_2 = 1:1

Table 4. Epoxidation of styrene monomer with H_2O_2 over Mo-SBA-15 as a function of reaction temperature

Temperature (°C)	Styrene conversion (%)	Selectivity (%)	
		Benzaldehyde	Styrene oxide
60	5.4	>99	-
70	6.3	70.9	29.1
80	42.1	84.5	15.5

Reaction condition: 0.05 g of 1.0 mol% Mo/styrene:H_2O_2 = 1:1

Table 5. Epoxidation of styrene monomer with H_2O_2 over Mo-SBA-15 as a function of ratio of styrene:H_2O_2

Ratio of styrene:H_2O_2	Styrene conversion (%)	Selectivity (%)	
		Benzaldehyde	Styrene oxide
1:0.5	7.5	72.7	27.3
1:1.0	6.3	70.9	29.1
1:1.5	9.1	72.7	27.3
1:2.0	5.5	69.1	30.8

Reaction condition: 0.05 g of 1.0 mol% Mo/70 °C/24 h

Table 6. Epoxidation of styrene monomer with H_2O_2 over Mo-SBA-15 as a function of catalyst used

Catalyst used (g)	Styrene conversion (%)	Selectivity (%)	
		Benzaldehyde	Styrene oxide
0.05	6.3	70.9	29.1
0.10	7.7	60.1	39.9
0.15	6.5	74.5	25.5

Reaction condition: 1.0 mol% Mo/70 °C/24 h/styrene:H_2O_2 = 1:1

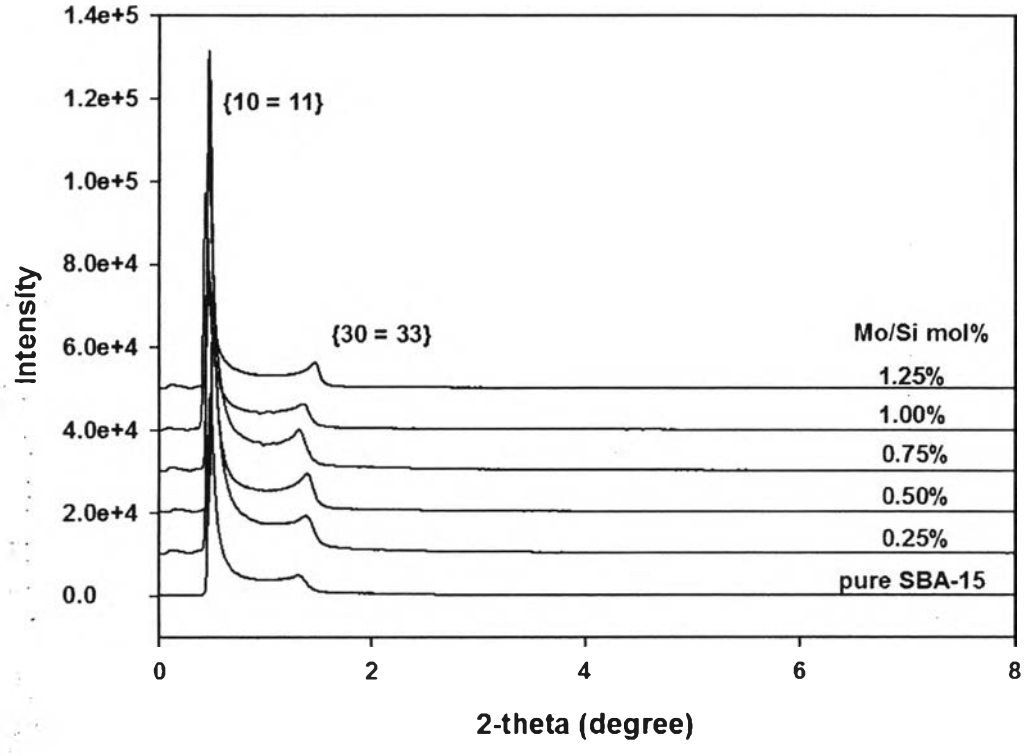

Figure 1 SAXS patterns of pure silica SBA-15 and Mo-SBA-15 containing different Mo loadings

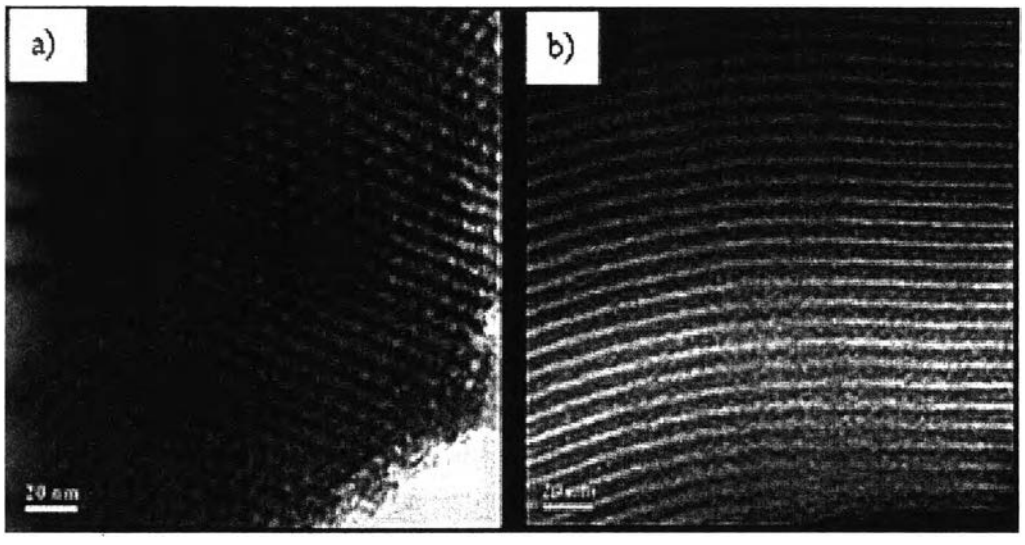

Figure 2 TEM images of Mo-SBA-15 containing 1.0 mol% Mo (A) in the direction perpendicular to the pore axis and (B) in the direction parallel to the pore axis

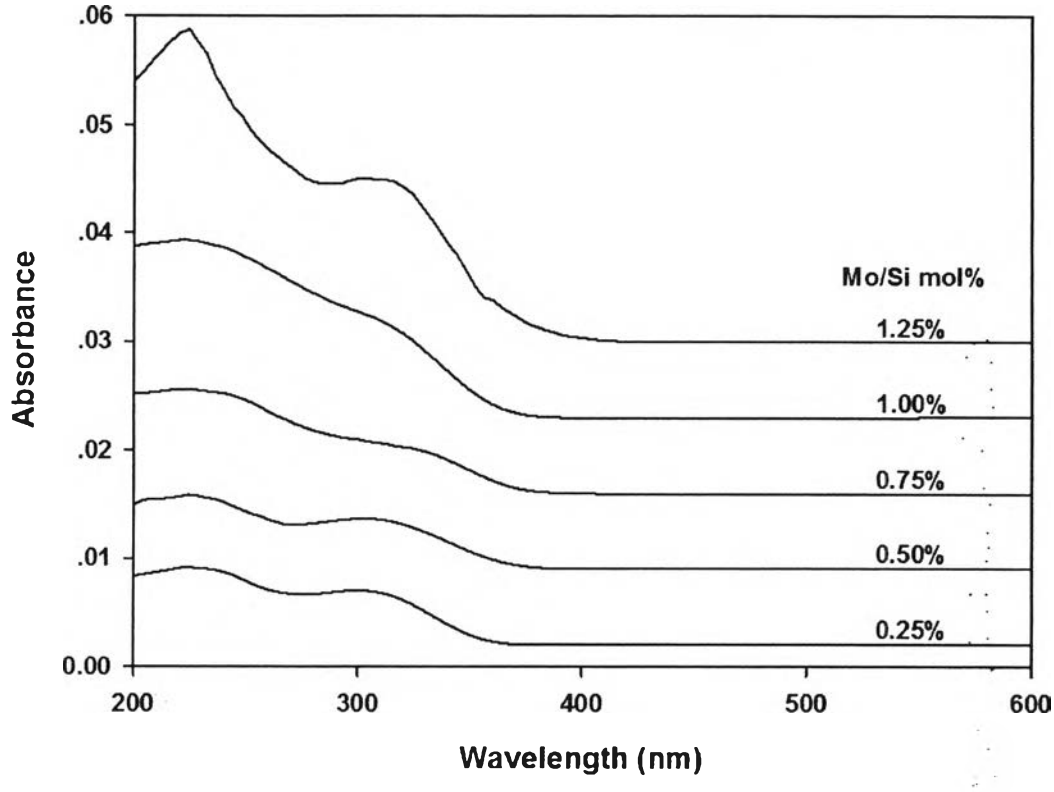

Figure 3 Diffuse reflectance UV-visible spectra of Mo-SBA-15

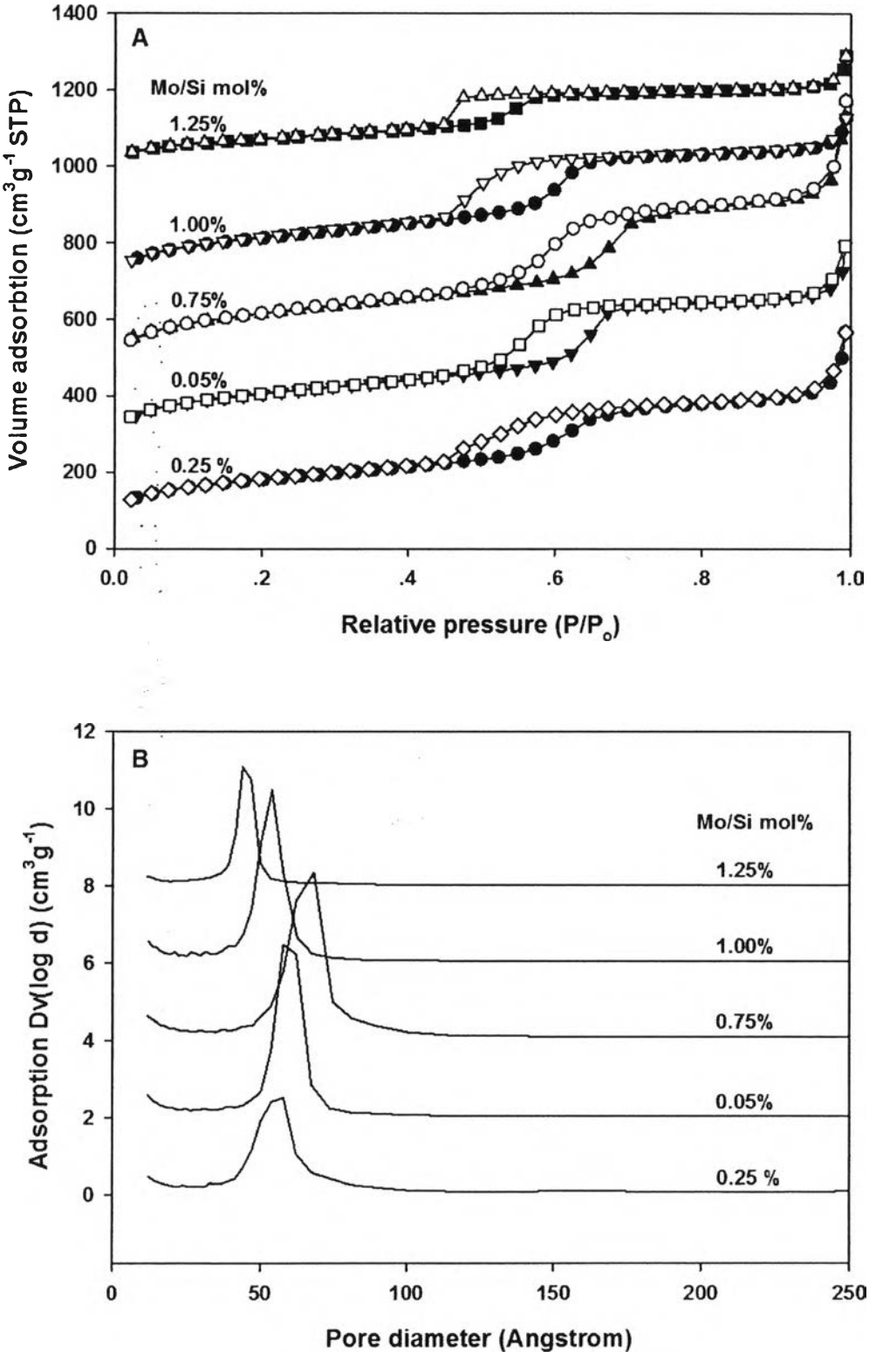

Figure 4 N_2 adsorption/desorption isotherms (A) and pore size distributions (B) of Mo-SBA-1